






## Research Article

# Experimental Study on the Ignition Sensitivity and Explosion Severity of Different Ranks of Coal Dust

Junfeng Wang <sup>1</sup>, Xiangbao Meng <sup>1,2,3</sup>, Yansong Zhang <sup>1,2</sup>, Haiyan Chen <sup>1,2</sup>,  
and Bo Liu <sup>1</sup>

<sup>1</sup>College of Mining and Safety Engineering, Shandong University of Science and Technology, Qingdao 266590, China

<sup>2</sup>Key Laboratory of Ministry of Education for Mine Disaster Prevention and Control, Shandong University of Science and Technology, Qingdao 266590, China

<sup>3</sup>Yankuang Group, Jining 273500, China

Correspondence should be addressed to Xiangbao Meng; [mxbsdust.edu.cn](mailto:mxbsdust.edu.cn)

Received 21 August 2019; Accepted 19 September 2019; Published 14 October 2019

Academic Editor: Zhixiong Li

Copyright © 2019 Junfeng Wang et al. This is an open access article distributed under the Creative Commons Attribution License, which permits unrestricted use, distribution, and reproduction in any medium, provided the original work is properly cited.

This study is conducted to examine the ignition sensitivity and explosion severity differences among different ranks of coal dust and reveal the causes underlying these differences. A G–G furnace, a Hartmann tube, and a 20 L explosion tank are used to test MIT, MIE,  $P_{\max}$ ,  $(dp/dt)_{\max}$ , and other parameters of three different ranks of coal dust. SEM analysis is carried out on the coal dust before and after explosion to compare and trace their microstructure changes. The results indicate that the lower the rank of the coal, the more likely the dust cloud to be ignited, the faster the explosion flame propagated, and the greater the explosion severity. The main drivers behind the ignition sensitivity and explosion severity differences among different ranks of coal dust are the volatile content and pyrolytic property of the coal.

## 1. Introduction

Coal is a conventional energy source with the highest reserve and the widest distribution in the world and one of the most important energy supplies across the globe [1]. Nevertheless, coal dust has long been threatening the exploitation, processing, and utilization of coal. Coal dust generation is unavoidable whether in coal mines, coal chemical plants, or coal-fired power generation facilities. The application of coal mining machinery in mining areas is more and more extensive [2, 3]. Although relevant mechanics research has been carried out [4], the intensity of coal mining has increased, and the amount of dust generated in coal mining face has increased. In semiclosed or closed spaces, coal dust tends to form dust clouds which, once exposed to ignition sources (electric sparks, open flames, or high-temperature heat sources), would explode and produce destructive shock waves which would raise the surrounding deposited coal dust and trigger a secondary explosion. Coal dust explosion

is generally highly destructive, since the explosion shock waves, burning flames, and high temperatures can lead to massive casualties and property damages [5]. For this reason, coal dust explosion studies have always been a highlight in the academic world.

The parameters to evaluate the risk of coal dust explosion mainly include ignition sensitivity parameters (MIE, MIT, and MEC) and explosion severity parameters ( $(P_{\max}, (dp/dt)_{\max})$ , and  $K_{St}$ ). Cashdollar [6] and Going et al. [7] studied the influence of dust concentration, particle size, and ambient temperature on explosion of different kinds of coal sample. Li et al. [8, 9] studied  $P_{\max}$  and  $(dp/dt)_{\max}$  after several coal dust sample explosions and analyzed them from the perspective of particle size distribution. This concurred with the conclusion of Liu et al. [10]. Using a 20 L and a 1 m<sup>3</sup> explosion tank, Man and Harris [11] studied the roles of large-sized coal dust in coal dust sample explosion and analyzed the  $P_{\max}$  and MEC. Using a vertical glass tube, Cao et al. [12, 13] examined the propagation property of coal dust

explosion flames with a high-speed camera. Using a 20 L explosion tank, Yuan et al. [14] investigated the roles of moisture in coal sample explosion and analyzed the explosion severity. Mishra and Azam [15] studied the MIT (concentration and particle size distribution) of coal dust clouds. Song et al. [16] investigated the mixed CH<sub>4</sub>/coal dust explosibility and its influencing factors and discovered that addition of CH<sub>4</sub> added to the coal dust severity. Wang et al. [17] studied how ignition delay time affected coal dust explosion.

Previous coal dust explosion results show that the risk of coal sample explosion is affected by many factors. However, restricted by experimental conditions or experimental purposes, few authors have approached the explosion proneness differences among different ranks of coal dust and the causes underlying these differences. MIE, MIT,  $P_{\max}$ , and  $(dP/dt)_{\max}$  of three coal samples with different metamorphic degrees were studied in this paper. We also discussed the causes underlying the explosion proneness differences among different ranks of coal dust by observing the particle microstructure before and after coal dust explosion.

## 2. Materials and Methods

**2.1. Coal Sample Preparation.** The three different coal dust used in our experiment, classified as lignite (HM), gas coal (QM), and anthracite (WY) according to their ranks, came from three different Chinese coal mines. As designed, these samples were crushed and passed through a 325-mesh standard metal wire sieve (GB/T6003.1-2012). Using Mastersizer 2000 laser particle size analyzer, we measured the particle size distribution of the coal dust samples after sieving. The result is listed in Figure 1. The particle size dispersity ( $\sigma_D$ ) was calculated using equation (1) [18]. The result indicated that the three coal dust samples had roughly the same median particle size ( $D_{50}$ ) and  $\sigma_D$ . Dry coal samples for 2 h in a dryer at 50°C to remove the moisture. The dried samples were then industrially analyzed using a WS-G818 automated industrial analyzer. The industrial analysis values are listed in Table 1.

$$\sigma_D = \frac{D_{90} - D_{10}}{D_{50}}. \quad (1)$$

Thermogravimetric analysis (TGA) is an important approach to examining the pyrolytic property of coal [19]. A thermogravimetric analyzer was used to analyze the pyrolytic property of the three coal dust samples. The heating rate was set to 10°C/min and a temperature range from room temperature to 800°C. The TG and DTG (derivative thermogravimetric) curves of the three coal dust samples are shown in Figure 2. At the low-temperature interval of below 100°C, the curves of all three samples displayed a marginal decline, caused by moisture losses in the samples. The appreciable decline of the TG curve of HM during this period precisely accorded with its high moisture content. As the temperature continued to rise, the TG curves of the three samples became flatter with limited mass losses. As the temperature further rose, the TG curves of all the samples began to decline remarkably with increasing mass loss rates

at all temperature points. The corresponding DTG curves also showed a strong spike. This period mainly marks the pyrolytic devolatilization of the coal dust samples and the combustion of fixed carbon. During this period, HM needed the lowest temperature to begin to lose mass, and its mass loss rate was the highest; QM needed a marginally higher temperature to begin to lose mass; and WY needed a significantly higher temperature to begin to lose mass. This suggests that there are some differences in the pyrolysis temperature and pyrolysis rate among the three different ranks of coal dust.

**2.2. Ignition Sensitivity Test and Flame Propagation Experiment.** The ambient temperature during the experiment was 25°C and the relative humidity was 38%. According to the MIT testing method for combustible dust cloud recommended in the Chinese National Standard GB/T 16429-1996, a Godbert–Greenwald (G–G) furnace (Figure 3) was used to test the MIT. This test apparatus includes a heating furnace, a dust storage chamber, a solenoid valve, an air storage chamber (with 0.5 L volume), a high-pressure gas cylinder, and an ignition temperature controller (with temperature range from room temperature to 1000°C). During the experiment, put a certain quantity of coal dust into the dust chamber and set the temperature. When the furnace temperature reaches the set temperature, the air storage chamber is pressurized to a certain pressure. Then start the solenoid valve. The dust cloud from the lower end of the heating furnace was observed at the same time to see if it was ignited. The mass of the coal sample ( $\leq 1$  g) and the dust spray pressure were changed according to the observation result until the highest temperature at which no ignition took place over ten repeated tests, which would be the MIT of the tested sample.

According to the MIE testing method for combustible dust cloud recommended in the Chinese National Standard GB/T 16428-1996, the MIE was tested using a Hartmann tube. This test apparatus is the same as that used in our previous study (which can produce 0.01–1000 J ignition energy) [5]. The pressure of the air storage chamber is set as 0.02 MPa. During the experiment, the dust cloud was observed to see whether it was ignited. Change sample quality ( $\leq 1$  g) according to whether the dust cloud was ignited until finding the highest ignition energy at which no ignition took place over 20 repeated tests, which would be the MIE of the tested coal dust sample. The Hartmann tube flame propagation experiment was carried out. In this process, 1 g of coal sample and 100 J of ignition energy were used.

**2.3. Explosibility Experiment.** Three coal dust samples were tested for explosive performance using a 20 L spherical explosion test system. This test system is the same as that used in our previous study [5]. The experiment was carried out according to the ASTM E1226 standard. To prevent overdrive in testing, the experiment used an ignition charge with 5 kJ energy [14]. The ignition head is made up of 40% zirconium, 30% barium nitrate, and 30% barium peroxide.

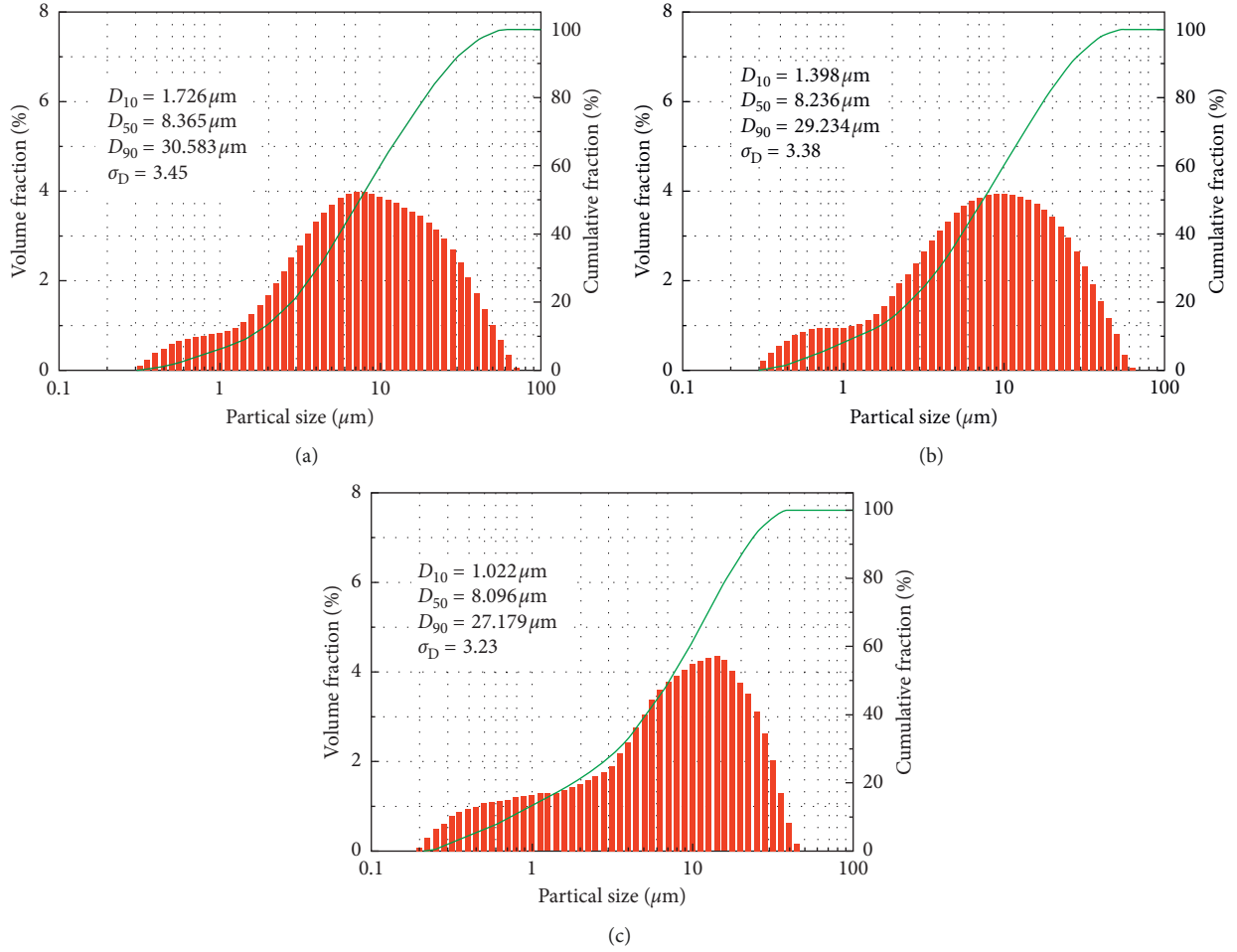


FIGURE 1: Particle size distribution: (a) HM; (b) QM; (c) WY.

TABLE 1: Proximate analyses of the coal samples.

Sample	Proximate analyses (wt.%)			
	$M_{ad}$	$A_{ad}$	$V_{daf}$	$FC_{ad}$
HM	11.39	4.55	42.26	48.54
QM	2.41	9.15	32.45	59.74
WY	1.05	22.75	11.19	67.67

$M_{ad}$ : moisture;  $A_{ad}$ : ash;  $V_{daf}$ : volatile matters;  $FC_{ad}$ : fixed carbon.

During the experiment, connect the ignition head to the ignition lead and close the explosion tank, and then add a certain quantity of coal sample. Vacuum the explosion tank to  $-0.06$  MPa, and the dust injection pressure is 2 MPa (gauge pressure). Then the solenoid valve is activated by the computer, and the coal dust is sprayed into the explosion tank. After 60 ms, the ignition head is ignited, and at the same time, the computer records the pressure data.

### 3. Results and Discussion

**3.1. Ignition Sensitivity and Flame Propagation of Different Ranks of Coal Dust.** MIT and MIE are important characteristic parameters for evaluating the ignition sensitivity of coal dust [20–22]. Table 2 presents the MIT and MIE test

results of the three different ranks of coal dust samples (HM, QM, and WY), although we were not able to obtain the MIE of WY within the maximum ignition energy achievable by the test apparatus (1000 J). From Table 2, the higher the rank of the coal, the higher the MIT and MIE of its dust cloud. HM and QM showed an MIT of  $520^{\circ}\text{C}$  and  $580^{\circ}\text{C}$ , respectively. The temperatures were relatively low and comparable; WY showed an MIT of  $880^{\circ}\text{C}$ , which is much higher than those of HM and QM. The MIE variations of the three samples were similar to their MIT variations. HM and QM showed an MIE of 2.5 J and 15.5 J, respectively, and WY showed an MIE higher than 1000 J. Ignition occurs to dust clouds because when dust particles are exposed to an amount of external energy, they will be pyrolytically devolatilized first; when the combustible volatile gases have arrived at a level of concentration, they will be ignited and will heat the surrounding dust particles, causing them to pyrolyze and burn. As can be observed from Figure 4, higher volatile contents in the dust coal samples will mean a lower MIT and MIE; volatile content constitutes an important driver for the ignition sensitivity of dust clouds. Meanwhile, the MIT and MIE of dust clouds are also associated with the pyrolytic property of coal dust samples. The less pyrolytic the coal dust is, the less likely the volatile matter is to be

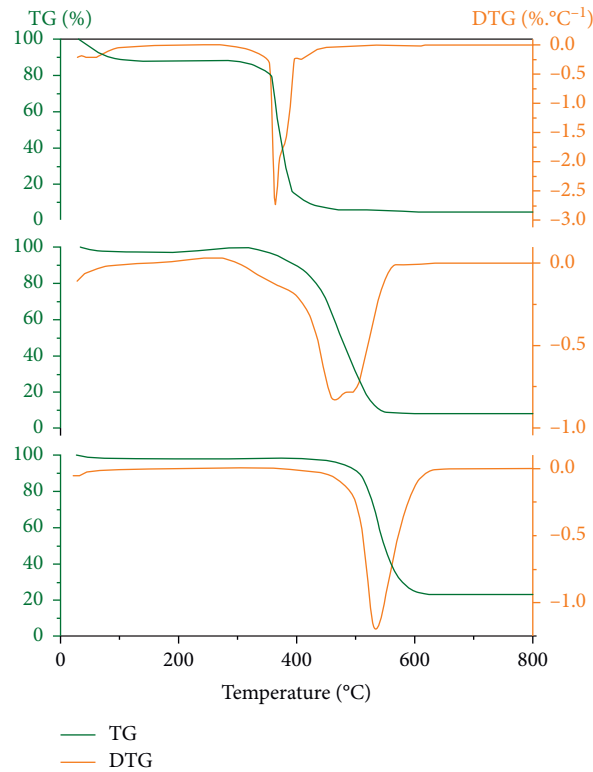


FIGURE 2: TG-DTG curves of the coal dust samples: (a) HM; (b) QM; (c) WY.

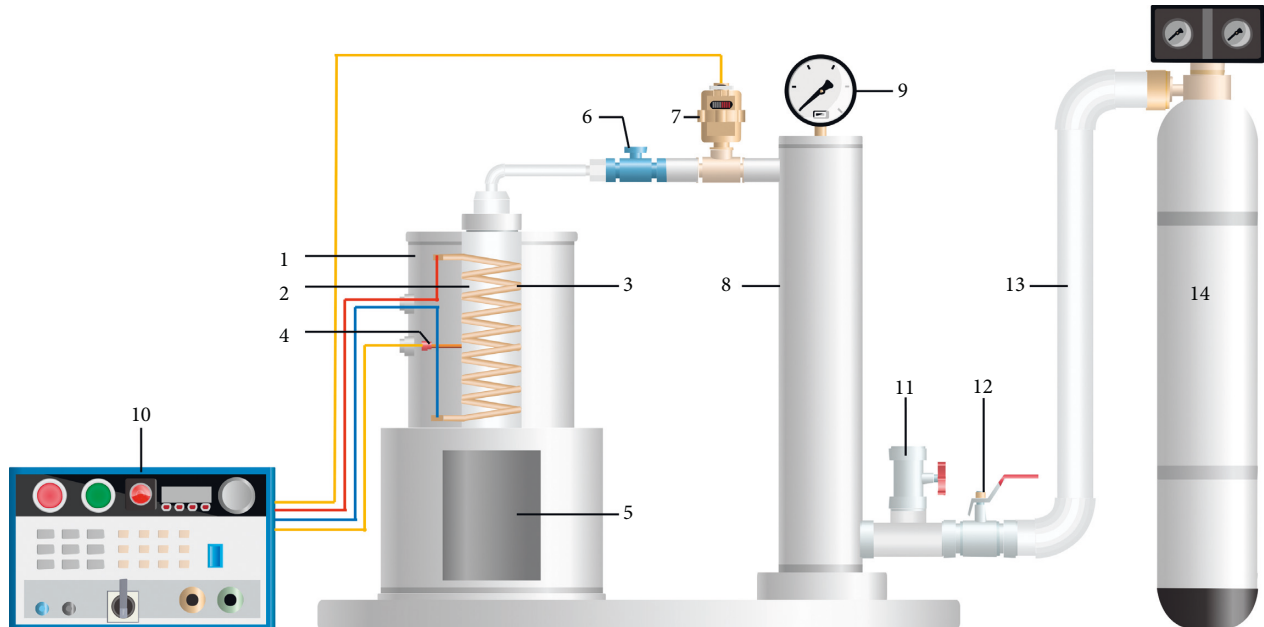


FIGURE 3: Godbert-Greenwald (G-G) furnace. 1, Heating furnace. 2, Quartz glass tube. 3, Resistive heater. 4, Thermocouple. 5, Sight glass. 6, Dust storage chamber. 7, Solenoid valve. 8, Air storage chamber. 9, Pressure Gauge. 10, Ignition temperature. 11, Exhaust valve. 12, Inlet valve. 13, High-pressure gas pipe. 14, High-pressure air cylinder controller.

TABLE 2: MIT and MIE of coal dust cloud.

Coal sample	HM	QM	WY
MIT (°C)	520	580	880
MIE (J)	2.5	15.5	>1000

precipitated and, consequently, the less likely the dust is to be ignited. The low-volatile content and relatively high pyrolysis temperature of WY and, consequently, its high MIT and MIE levels, prevented the dust cloud from being readily ignited. The test results of MIT in this paper are

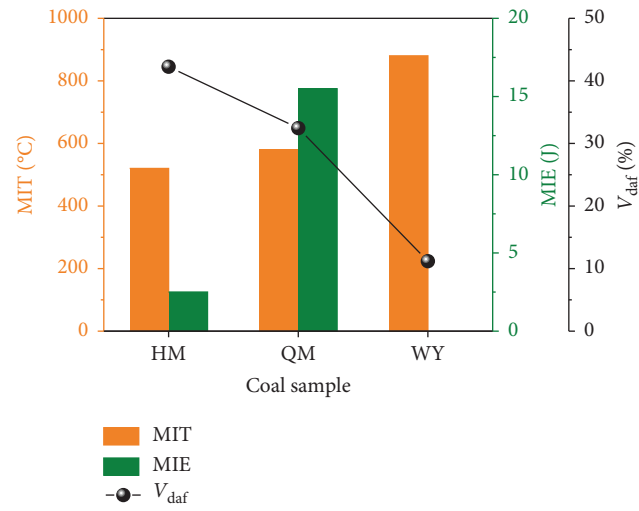


FIGURE 4: MIT, MIE, and volatile matter of the three coal dust samples.

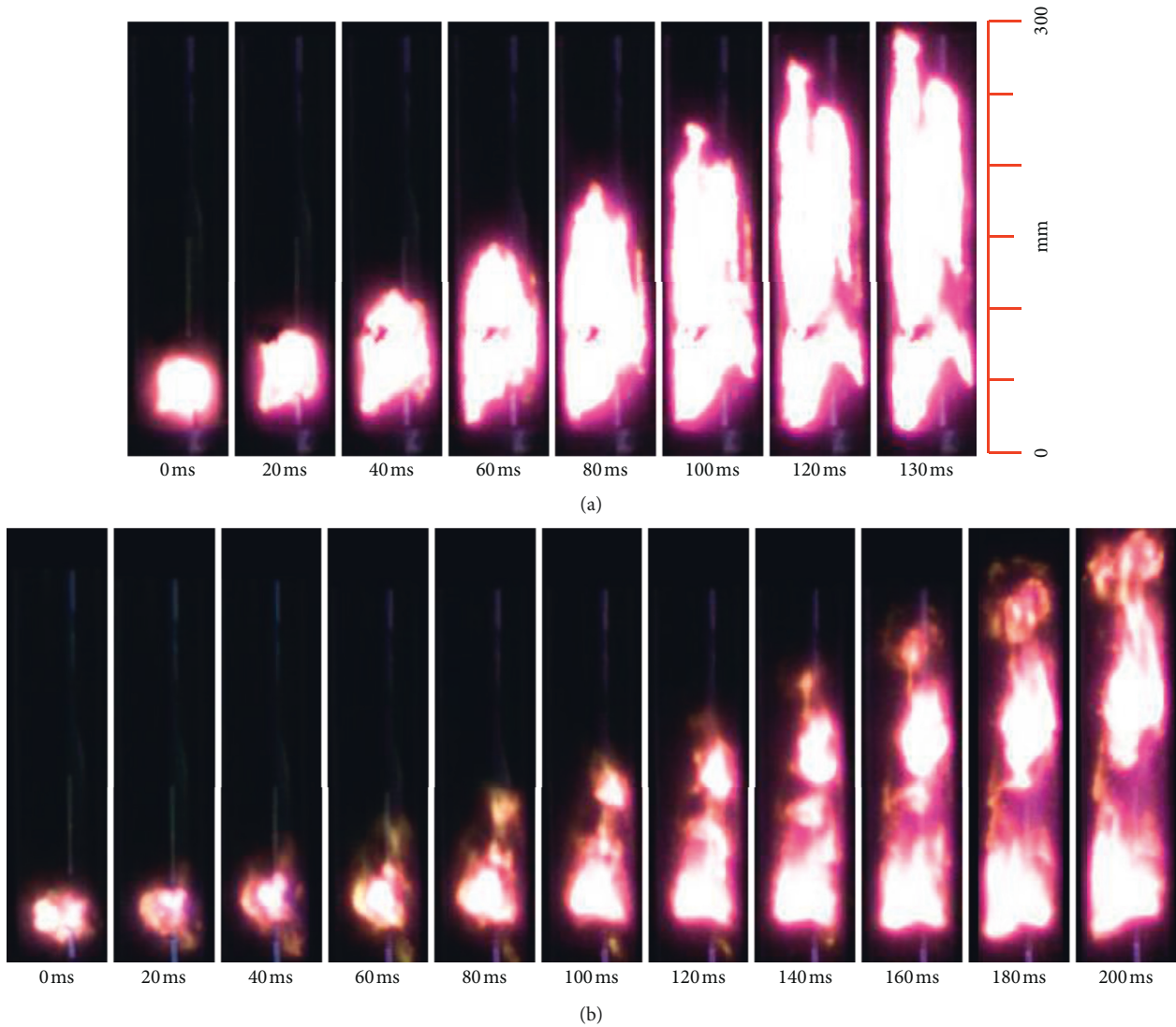


FIGURE 5: Photographs of the flame propagation: (a) HM; (b) QM.

different from those in the literature [15], mainly due to different types of coal dust samples and different treatment methods.

Figure 5 shows the flame propagation processes of the HM and QM dust clouds after ignited in a 300 mm long vertical glass tube. From this photograph, the QM dust cloud took 200 ms to be propagated to the top of the glass tube after ignition, whereas the HM dust cloud took merely 130 ms, which is more than 70 ms shorter. This suggests that the average flame propagation velocity of the HM was remarkably higher than that of the QM, primarily because the high volatile content and high pyrolysis velocity of HM allowed rapid pyrolysis and precipitation of large amounts of volatile matter after the dust particles were heated, making flame propagation even faster. Furthermore, from this photograph, the HM flames were brighter than the QM flames, suggesting that the HM was burning more violently, possibly because of its high volatile content, too.

**3.2. Explosibility of Different Ranks of Coal Dust.** The main parameters used to evaluate the explosibility of dust are the maximum explosion pressure ( $P_{\max}$ ), maximum explosion pressure rise rate ( $(dP/dt)_{\max}$ ), and burning time ( $t_b$ ) [5]. Burning time ( $t_b$ ) refers to the time when the dust cloud reaches the  $P_{\max}$  after ignition. [23] Explosion index ( $K_{St}$ ) refers to the  $(dP/dt)_{\max}$  in a 1 m<sup>3</sup> explosion tank, which can be calculated according to equation (2). The  $K_{St}$  value measured from the 20 L spherical explosion tank is an important parameter for explosion-proof design of installations [24–26]:

$$K_{St} = \left( \frac{dp}{dt} \right)_{\max} \cdot V^{1/3}. \quad (2)$$

Three kinds of coal samples (HM, QM, and WY) were tested on four different mass concentrations (125 g/m<sup>3</sup>, 250 g/m<sup>3</sup>, 375 g/m<sup>3</sup>, and 500 g/m<sup>3</sup>). Table 3 shows the explosibility parameters of the coal dust samples. Figure 6 shows the measured explosion pressure histories of the samples. During dust cloud explosion, the dust particles near the ignition source were first heated and pyrolytically devolatilized. Near the ignition source, mixtures of volatile gases, and coal char were formed. The ignition source ignited the precipitated combustible volatile gases. The explosion pressure began to rise. The gas-phase burning flames continued to heat the coal char and the surrounding unburnt dust particles, triggering heterogeneous combustion of the volatile gases and coal char which gave rise to thermal decomposition of the coal dust. The burning flames spread outward. By the time the burning flames reached the vessel wall, the combustible matter and oxygen content had been gradually consumed. The burning reaction rate gradually decreased. After the maximum explosion pressure was reached, the burning reaction ended, and as a result of avoiding heat dissipation of the explosion tank, the explosion pressure began to attenuate. The  $P_{\max}$  of WY is 0.074 MPa at the concentration of 125 g/m<sup>3</sup>. Hence, this curve was mainly caused by the explosion of the ignition head, and no explosion took place in the dust cloud [27].

This demonstrates that the WY dust cloud had a minimum explosion concentration (MEC) higher than 125 g/m<sup>3</sup>, primarily because WY had a low-volatile content and was hardly pyrolytic. As a result, at low concentrations, the pyrolyzed combustible volatile gases were limited. This made it hard for the dust cloud to be readily ignited, thereby giving rise to a high MEC.

Figure 7 shows how the  $P_{\max}$ ,  $(dP/dt)_{\max}$ , and  $t_b$  of the three different ranks of coal dust related to dust concentration. From Figure 7(a), the maximum explosion pressures of the three coal dust samples were: HM > QM > WY. That is, lower ranks of coal dust produced higher maximum explosion pressures. With the increase of dust concentration, the  $P_{\max}$  of all three samples displayed an increase-and-decrease trend. This is because at low concentrations, the main constraint on the  $P_{\max}$  is the content of combustible matter (coal dust). At a given concentration, with the increase of concentration, the combustible composition also increases, causing the  $P_{\max}$  to increase. However, after exceeding a certain concentration, restricted by the oxygen content, the dust is not completely burnt after the dust concentration is increased. The nonburning part of the dust particles will absorb part of the burning heat, thereby reducing the  $P_{\max}$ . It is noted, however, that both HM and QM reached their maximum  $P_{\max}$ , 0.514 MPa and 0.5 MPa, at 250 g/m<sup>3</sup>, whereas WY did not reach its maximum  $P_{\max}$  until at 375 g/m<sup>3</sup>. This is because WY had a very low-volatile content. From Figure 7(b), obviously, the order of the  $(dP/dt)_{\max}$  is: HM > QM > WY. That is, lower ranks of coal dust have higher  $(dP/dt)_{\max}$ . This is attributable to the different volatile contents in the coal dust. The  $(dP/dt)_{\max}$  tended to rise and then flatten with the increased concentration. This is because the higher the concentration of coal dust, the higher the content of volatile matter precipitated and the higher the burning reaction rate, but, at a given level of concentration, again, restricted by the oxygen concentration, the burning rate will not be always increasing. From Figure 7(c), the burning times of the three coal dust samples were: WY > QM > HM. That is, lower ranks of coal dust take a shorter time to burn. This corresponds with the  $(dP/dt)_{\max}$ : The higher the  $(dP/dt)_{\max}$ , shorter the burning time. In terms of the  $(K_{St})_{\max}$  of the coal dust, HM had the highest  $(K_{St})_{\max}$  at 14.66 MPa·m/s, followed by QM at 9.77 MPa·m/s; WY had the lowest  $(K_{St})_{\max}$  at 4.83 MPa·m/s. Li et al. [8] also tested the explosibility of several coal dust particles. The  $(K_{St})_{\max}$  of Neimeng coal ( $V_{daf} = 14.03\%$ ) was 7.49 MPa·m/s, the  $(K_{St})_{\max}$  of Ningxia coal ( $V_{daf} = 33.51\%$ ) was 24.77 MPa·m/s, and the  $(K_{St})_{\max}$  of Huaibei coal ( $V_{daf} = 35.77\%$ ) is 31.00 MPa·m/s.

**3.3. SEM Analysis of Coal Sample.** The postexplosion residue of dust represents an important basis for investigating the dust explosion process [28, 29]. In order to explore the causes underlying the differences in the explosibility parameters among different ranks of coal dust, a scanning electron microscope (SEM) that can observe the microstructure of the three raw coal samples and their products

TABLE 3: Explosibility parameters of coal dust.

Coal sample	$C_{\text{dust}}$ ( $\text{g}/\text{m}^3$ )	$P_{\text{max}}$ (MPa)	$(dP/dt)_{\text{max}}$ (MPa/s)	$t_b$ (ms)	$K_{\text{St}}$ (MPa·m/s)
HM	125	0.431	12.3	65	3.34
	250	0.514	28.5	29	7.74
	375	0.479	54	17	14.66
	500	0.452	52.8	18	14.33
QM	125	0.412	7.67	119	2.08
	250	0.5	19.5	57	5.29
	375	0.465	36	37	9.77
	500	0.424	33.6	36	9.12
WY	125	—	—	—	—
	250	0.42	9.3	89	2.52
	375	0.448	16.6	67	4.51
	500	0.423	17.8	55	4.83

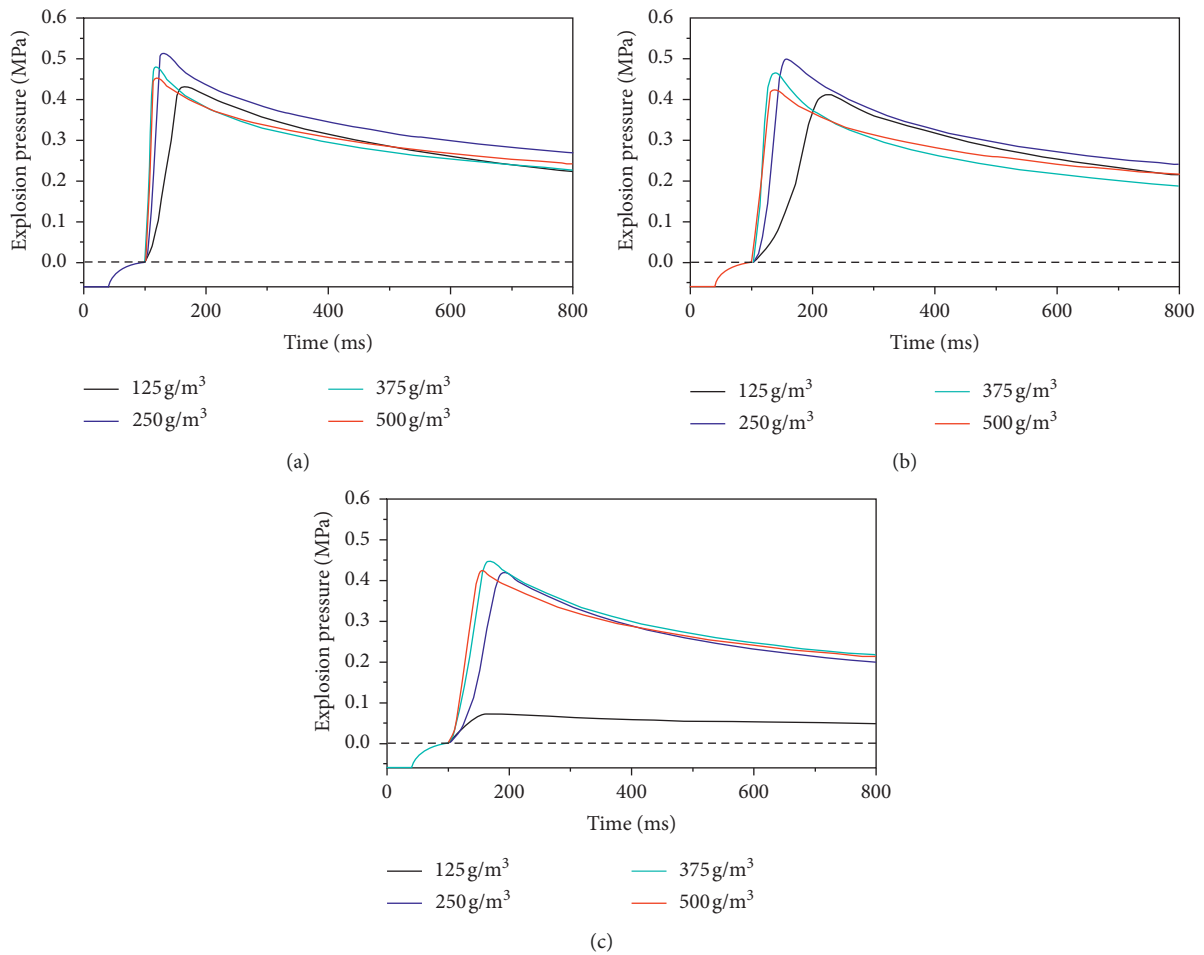


FIGURE 6: Explosion pressure time history of the three coal dust samples under different concentrations: (a) HM; (b) QM; (c) WY.

after explosion is used. The SEM images of coal dust before and after explosion are shown in Figure 8.

From these images, we can clearly see that before explosion, the particles of the three raw coal dust samples were unequal in size and irregular in shape, with obvious edges and angles, relatively smooth surfaces, and no visible pore structure. After explosion, most of the dust particles lost

their edges and angles; some of the particles showed quite many folds and quite many visible pore structures on their surfaces; and the explosion products also contained a few broken spherical shell-like fragments, which consisted of the part of the dust particles that were more completely burned during the explosion. They also contained particles that were morphologically similar to the pre-explosion dust particles,

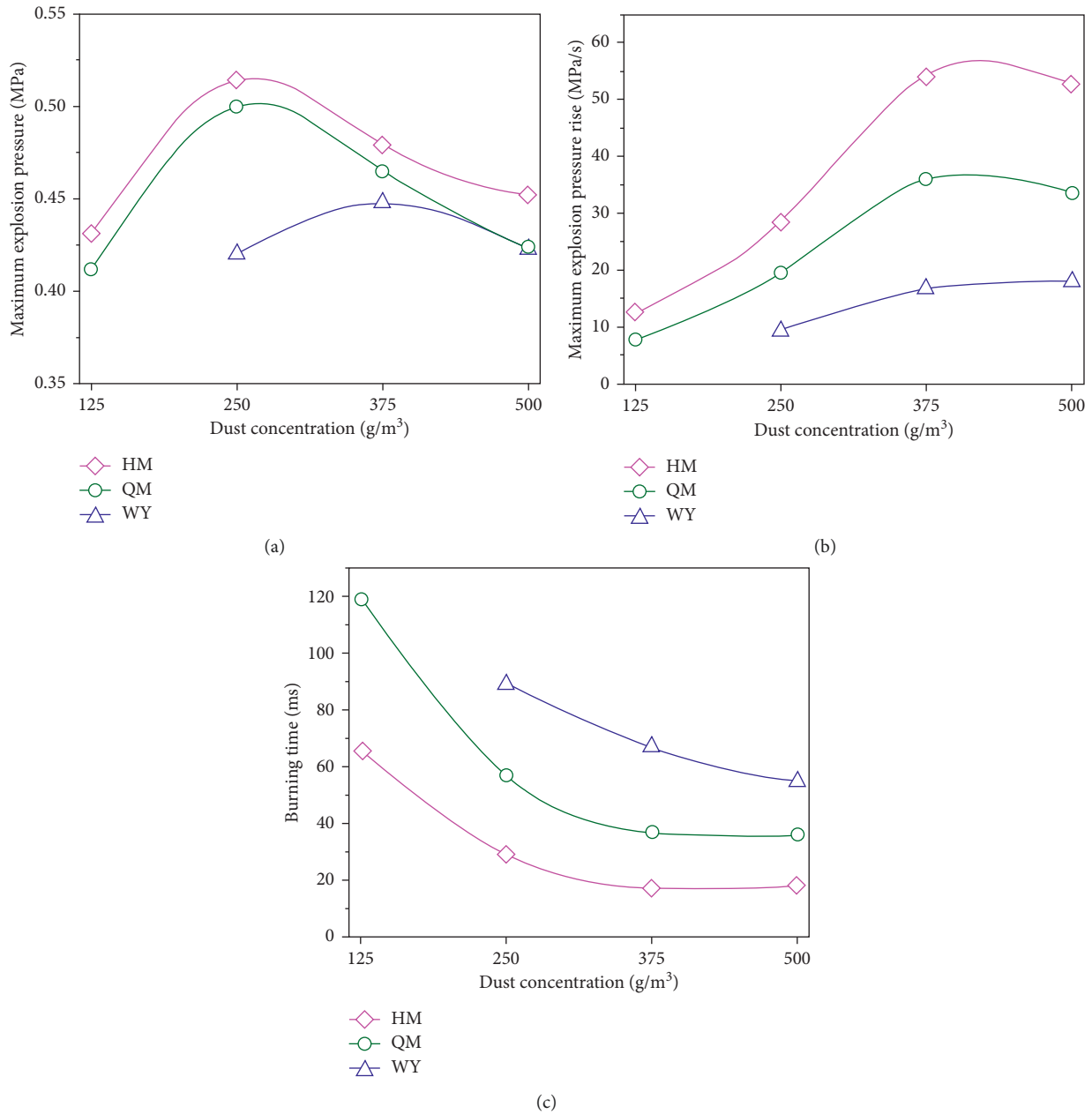


FIGURE 7:  $P_{\max}$ ,  $(dP/dt)_{\max}$ , and  $t_b$  of the three coal dust under different concentrations: (a) HM; (b) QM; (c) WY.

suggesting that these particles were not involved in this burning process. The postexplosion product of HM contained particles with obviously large and deep pores and some broken spherical shell-like fragments, suggesting that the burning reaction was quite complete; the postexplosion product of WY showed smaller pores in the particles and contained quite many nonburning particles, suggesting that the burning reaction was very incomplete.

Figure 9 shows the burning reaction and structural evolution process of the coal particles during coal sample explosion. After coal sample particles are heated, the coal particles were first pyrolyzed. The volatile matter precipitated from inside of the coal particles through fine pores. The gas-phase burning reaction of the combustible volatile

matter so precipitated formed porous coal char. Then, the fixed carbon fraction of the porous coal char continued to participate in the burning reaction. Burning of the solid phase of the coal char caused the angles on the particle surfaces to disappear and the pores to enlarge. When exposed to heat stresses and explosion shock waves, the particles where the coal char was more completely burnt formed broken spherical shell-like fragments. HM, with a relatively high-volatile content, was the most readily pyrolyzed. As participation of large amounts of volatile matter in the burning can release large amounts of heat and the gas-phase burning flames can stimulate the solid-phase burning of coal char, the particles were quite completely burnt during the explosion, giving rise to a relatively high  $P$ , and  $P_{\max}$ .



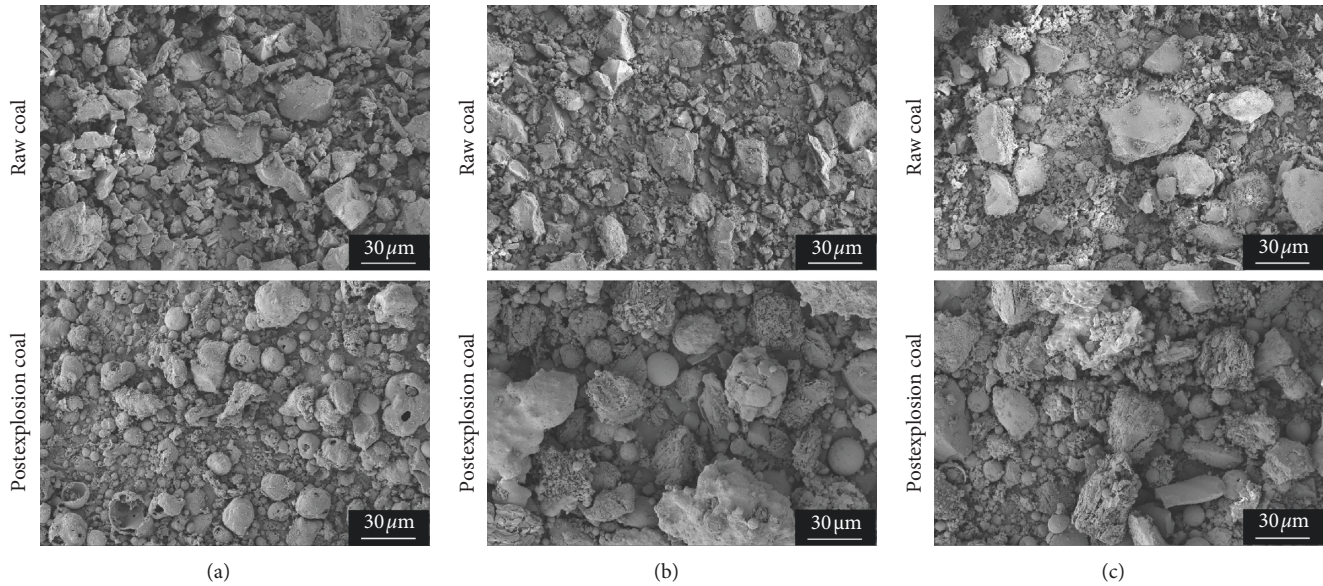


FIGURE 8: SEM images of the coal dust and their postexplosion products: (a) HM; (b) QM; (c) WY.

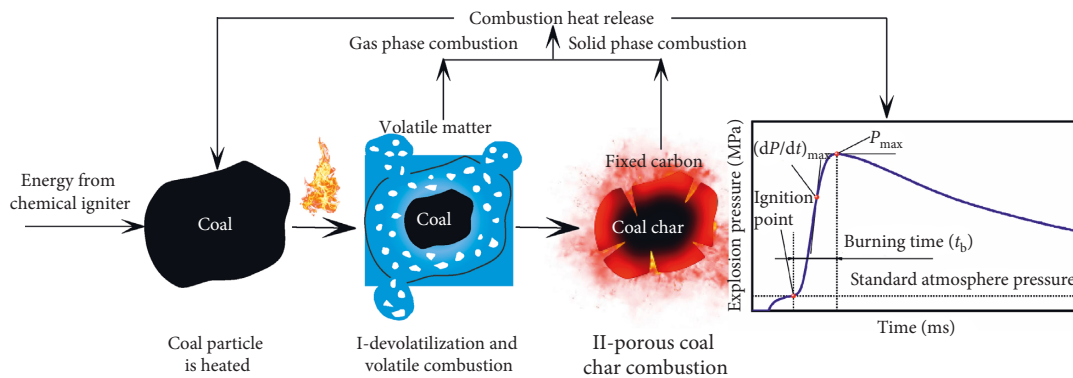


FIGURE 9: Explosion mechanism of the coal dust.

WY, with a very low-volatile content, was less readily pyrolyzed. The relatively weak gas-phase burning caused the coal particles to be incompletely burned during the explosion. Some particles were even not pyrolyzed at all. This resulted in a relatively low explosion pressure and explosion pressure rise rate.

#### 4. Conclusions

The MIT and MIE of three different ranks of coal dust were measured with a G-G furnace. The result indicated that higher ranks of coal have a higher MIT and MIE and the dust cloud is less readily ignited. This should be attributable to the different volatile contents and pyrolysis properties among different ranks of coal sample. The coal sample that has a high volatile content and is easily pyrolyzed has a lower MIT and MIE, the dust cloud is more readily ignited and flames developed more rapidly at the beginning of explosion.

Using a 20 L explosion tank, the explosion severity of the three different ranks of coal dust was examined, with focuses

on the  $P_{\max}$ ,  $(dP/dt)_{\max}$ ,  $t_b$ , and  $K_{St}$ . The result indicated that as the concentration increased, all three samples displayed an increase-and-decrease  $P_{\max}$  variation; both HM and QM reached their maximum  $P_{\max}$  at  $250 \text{ g/m}^3$ , whereas WY did not reach its  $250 \text{ g/m}^3$  until at  $375 \text{ g/m}^3$ , and it did not explode when the concentration was  $<125 \text{ g/m}^3$ . Lower ranks of coal sample have a higher  $P_{\max}$ ,  $(dP/dt)_{\max}$ , and  $K_{St}$  and smaller  $t_b$ . That is, they have a higher explosion severity.

The coal dust explosion mechanism was investigated by observing the microstructure of coal dust. During the explosion, the coal particles were first pyrolytically devolatilized, leading to volatile matter burning and then the burning of the coal char. The gas-phase burning flames will enhance the burning of coal char, causing the dust particles to be more completely burnt. The main driver underlying the explosion severity differences among different ranks of coal is the precipitation velocity of the volatile. The coal dust that has higher volatile contents and is easier pyrolyzed has a higher volatile precipitation rate, a higher burning reaction rate, a higher burning completeness for the dust particles, and a higher explosion severity.

## Data Availability

The data used to support the findings of this study are available from the corresponding author upon request.

## Conflicts of Interest

The authors declare that there are no conflicts of interest regarding the publication of this paper.

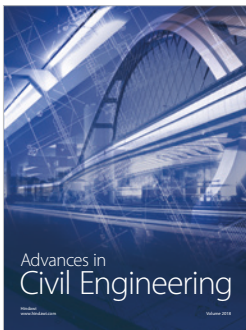
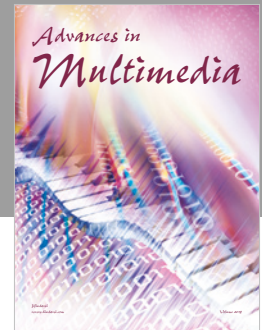
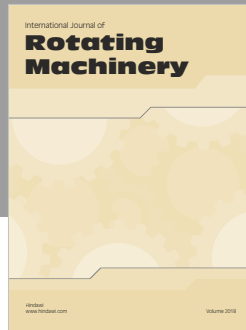
## Acknowledgments

This research was funded by the Key Research and Development project of Shandong Province (2018GSF120016 and 2018GGX109004), the National Key Research and Development Plan (2017YFC0805200 and 2016YFC0801700), and the China Postdoctoral Science Foundation (2018M632693).

## References

- [1] X. Li, S. Wang, S. Ge, R. Malekian, Z. Li, and Y. Li, "A study on drum cutting properties with full-scale experiments and numerical simulations," *Measurement*, vol. 114, pp. 25–36, 2018.
- [2] L. Xuefeng, W. Shibo, G. Shirong, R. Malekian, and L. Zhixiong, "Investigation on the influence mechanism of rock brittleness on rock fragmentation and cutting performance by discrete element method," *Measurement*, vol. 113, pp. 120–130, 2018.
- [3] X. Li, S. Wang, S. Ge, R. Malekian, and Z. Li, "A theoretical model for estimating the peak cutting force of conical picks," *Experimental Mechanics*, vol. 58, no. 5, pp. 709–720, 2018.
- [4] S. Z. Feng, S. P. A. Bordas, X. Han, G. Wang, and Z. X. Li, "A gradient weighted extended finite element method (GW-XFEM) for fracture mechanics," *Acta Mechanica*, vol. 230, no. 7, pp. 2385–2398, 2019.
- [5] J. Wang, X. Meng, X. Ma, Q. Xiao, B. Liu, and G. Zhang, "Experimental study on whether and how particle size affects the flame propagation and explosibility of oil shale dust," *Process Safety Progress*, vol. 38, no. 3, Article ID e12075, 2019.
- [6] K. L. Cashdollar, "Overview of dust explosibility characteristics," *Journal of Loss Prevention in the Process Industries*, vol. 13, no. 3–5, pp. 183–199, 2000.
- [7] J. E. Going, K. Chatrathi, and K. L. Cashdollar, "Flammability limit measurements for dusts in 20-L and 1-m<sup>3</sup> vessels," *Journal of Loss Prevention in the Process Industries*, vol. 13, pp. 209–219, 2000.
- [8] Q. Z. Li, C. C. Yuan, Q. L. Tao, Y. N. Zheng, and Y. Zhao, "Experimental analysis on post-explosion residues for evaluating coal dust explosion severity and flame propagation behaviors," *Fuel*, vol. 215, pp. 417–428, 2018.
- [9] Q. Z. Li, K. Wang, Y. N. Zheng, M. L. Ruan, X. N. Mei, and B. Q. Lin, "Experimental research of particle size and size dispersity on the explosibility characteristics of coal dust," *Powder Technology*, vol. 292, pp. 290–297, 2016.
- [10] S. H. Liu, Y. F. Cheng, X. R. Meng et al., "Influence of particle size polydispersity on coal dust explosibility," *Journal of Loss Prevention in the Process Industries*, vol. 56, pp. 444–450, 2018.
- [11] C. K. Man and M. L. Harris, "Participation of large particles in coal dust explosions," *Journal of Loss Prevention in the Process Industries*, vol. 27, pp. 49–54, 2014.
- [12] W. G. Cao, W. Gao, J. Y. Liang, S. Xu, and F. Pan, "Flame-propagation behavior and a dynamic model for the thermal-radiation effects in coal-dust explosions," *Journal of Loss Prevention in the Process Industries*, vol. 29, pp. 65–71, 2014.
- [13] W. G. Cao, W. Gao, Y. H. Peng, J. Y. Liang, F. Pan, and S. Xu, "Experimental and numerical study on flame propagation behaviors in coal dust explosions," *Powder Technology*, vol. 266, pp. 456–462, 2014.
- [14] J. J. Yuan, W. Y. Wei, W. X. Huang, B. Du, L. Liu, and J. H. Zhu, "Experimental investigations on the roles of moisture in coal dust explosion," *Journal of the Taiwan Institute of Chemical Engineers*, vol. 45, pp. 2325–2333, 2014.
- [15] D. P. Mishra and S. Azam, "Experimental investigation on effects of particle size, dust concentration and dust-dispersion-air pressure on minimum ignition temperature and combustion process of coal dust clouds in a G-G furnace," *Fuel*, vol. 227, pp. 424–433, 2018.
- [16] S. X. Song, Y. F. Cheng, X. R. Meng et al., "Hybrid CH<sub>4</sub>/coal dust explosions in a 20-L spherical vessel," *Process Safety and Environmental Protection*, vol. 122, pp. 281–287, 2019.
- [17] S. Y. Wang, Z. C. Shi, X. Peng et al., "Effect of the ignition delay time on explosion severity parameters of coal dust/air mixtures," *Powder Technology*, vol. 342, pp. 509–516, 2019.
- [18] D. Castellanos, V. H. Carreto-Vazquez, C. V. Mashuga, R. Trotter, A. F. Mejia, and M. S. Mannan, "The effect of particle size polydispersity on the explosibility characteristics of aluminum dust," *Powder Technology*, vol. 254, pp. 331–337, 2014.
- [19] W. Z. Du, G. Wang, Y. Wang, and X. L. Liu, "Thermal degradation of bituminous coal with both model-free and model-fitting methods," *Applied Thermal Engineering*, vol. 152, pp. 169–174, 2019.
- [20] E. K. Addai, D. Gabel, and U. Krause, "Experimental investigations of the minimum ignition energy and the minimum ignition temperature of inert and combustible dust cloud mixtures," *Journal of Hazardous Materials*, vol. 307, pp. 302–311, 2016.
- [21] E. K. Addai, D. Gabel, and U. Krause, "Experimental investigation on the minimum ignition temperature of hybrid mixtures of dusts and gases or solvents," *Journal of Hazardous Materials*, vol. 301, pp. 314–326, 2016.
- [22] H. Sun, Y. Pan, J. Guan et al., "Thermal decomposition behaviors and dust explosion characteristics of nano-polystyrene," *Journal of Thermal Analysis and Calorimetry*, vol. 135, pp. 2359–2366, 2019.
- [23] Q. Z. Li, B. Q. Lin, H. M. Dai, and S. Zhao, "Explosion characteristics of H<sub>2</sub>/CH<sub>4</sub>/air and CH<sub>4</sub>/coal dust/air mixtures," *Powder Technology*, vol. 229, pp. 222–228, 2012.
- [24] T. Abbasi and S. A. Abbasi, "Dust explosions—Cases, causes, consequences, and control," *Journal of Hazardous Materials*, vol. 140, no. 1–2, pp. 7–44, 2007.
- [25] A. Fumagalli, M. Derudi, R. Rota, and S. Copelli, "Estimation of the deflagration index  $K_{St}$  for dust explosions: a review," *Journal of Loss Prevention in the Process Industries*, vol. 44, pp. 311–322, 2016.
- [26] A. Fumagalli, M. Derudi, R. Rota, J. Snoeys, and S. Copelli, "A kinetic free mathematical model for the prediction of the  $K_{St}$  reduction with the particle size increase," *Journal of Loss Prevention in the Process Industries*, vol. 52, pp. 93–98, 2018.
- [27] L. F. Yu, G. Li, W. C. Liu, J. N. Yu, and C. M. Yuan, "Experimental investigations on ignition sensitivity of hybrid mixtures of oil shale dust and syngas," *Fuel*, vol. 210, pp. 1–7, 2017.
- [28] H. S. Sen, Z. T. Liu, E. L. Zhao et al., "Comparison of behavior and microscopic characteristics of first and secondary

- explosions of coal dust,” *Journal of Loss Prevention in the Process Industries*, vol. 49, pp. 382–394, 2017.
- [29] Z. T. Liu, S. Lin, S. S. Zhang, E. Y. Wang, and G. H. Liu, “Observations of microscopic characteristics of post-explosion coal dust samples,” *Journal of Loss Prevention in the Process Industries*, vol. 43, pp. 378–384, 2016.



**Hindawi**

Submit your manuscripts at  
[www.hindawi.com](http://www.hindawi.com)

